Tests of a 2D Diamond Differences S_N Code

Erik Hansen

May 5, 2025

1 Simulation Design

1.1 Transport Sweep

We write the 3D transport equation with isotropic source and scattering as [2]

$$\Omega \cdot \nabla \psi + \Sigma_t \psi = \frac{1}{4\pi}\left(Q_0 + \Sigma_s \phi\right) \tag{1}$$

with symmetry in the $\hat{z}$ direction as

$$\mu \frac{\partial \psi}{\partial x} + \sqrt{1-\mu^2}\cos\phi \frac{\partial \psi}{\partial y} + \Sigma_t \psi = \frac{1}{4\pi}\left(Q_0 + \Sigma_s \phi\right) \tag{2}$$

where $\mu = \cos\theta$ with ϕ the angle between the direction of neutron travel and the x axis and $\phi \in [-\pi, \pi]$ the angle in the yz plane between the direction of neutron travel and the y axis. Given the symmetry in z, we also have a symmetry as $\theta, \phi \to -\theta, -\phi$, so we can only consider positive ϕ and reduce this equation to

$$\mu \frac{\partial \psi}{\partial x} + \sqrt{1-\mu^2}\cos\phi \frac{\partial \psi}{\partial y} + \Sigma_t \psi = \frac{1}{2\pi}\left(Q_0 + \Sigma_s \phi\right) \tag{3}$$

Now we discretize in space following Lewis and Miller using the finite volume and diamond difference method, which models the value of ψ in a cell as the average of the value at the four cell nodes and the value of ψ at a cell edge as the average of the two nodes. [3] Integrating in space yields the following equation for the node values $\psi_{i,j}$

$$\begin{aligned}
&\left(\frac{\mu}{2}\Delta y + \frac{\sqrt{1-\mu^2}\cos\phi}{2}\Delta x + \frac{\Sigma_t}{4}\Delta x \Delta y\right)\psi_{i+1,j+1} \\
&+\left(-\frac{\mu}{2}\Delta y + \frac{\sqrt{1-\mu^2}\cos\phi}{2}\Delta x + \frac{\Sigma_t}{4}\Delta x \Delta y\right)\psi_{i,j+1} \\
&+\left(\frac{\mu}{2}\Delta y - \frac{\sqrt{1-\mu^2}\cos\phi}{2}\Delta x + \frac{\Sigma_t}{4}\Delta x \Delta y\right)\psi_{i+1,j} \\
&+\left(-\frac{\mu}{2}\Delta y - \frac{\sqrt{1-\mu^2}\cos\phi}{2}\Delta x + \frac{\Sigma_t}{4}\Delta x \Delta y\right)\psi_{i,j} = \frac{1}{2\pi}\left(Q_0 + \Sigma_s \phi\right)
\end{aligned} \tag{4}$$

Given μ and ϕ, we can then solve this equation from left to right, or right to left, and bottom to top, or top to bottom, according to the sign of μ and $\cos\phi$.[3] We now choose a product quadrature where μ and $\frac{\phi}{\pi} - 1$ lie on Gaussian quadrature points in $[-1, 1]$ and corresponding weights to integrate the angular flux to find the scalar flux. Upon this choice, the transport equation is solved via the source iteration method.[1]

1.2 Selection of Problems

We first choose to validate our solution by studying a medium which is an isotropic source with scattering and isotropic boundary conditions. This benchmarking problem is chosen because it has a known solution and predicted form.

After this, we seek out pathological situations which emerge to test the ability of our diamond difference code to resolve important features. In analogy to the example of a central source that was discussed in class, we test a problem with four sources central to the corners of an absorbing medium with $\Sigma_t = 1$ and $\Sigma_s = 0.2$. We expect to see ray effects here due to localized sources and an absorbing medium. As an example of an incoming flux problem, we construct a wide beam of the largest μ entering the domain of air with $\Sigma_t = 0.01$ and $\Sigma_s = 0.006$. We might think of this problem as open door for neutrons moving in one direction on one side of the domain and observing the spread of neutrons. This problem may also experience ray effects due to the highly localized source.

We also seek to demonstrate false diffusion through these examples. Based on the discussion of the shadow of a building appearing to diffuse and not being clear, we construct an absorber with $\Sigma_t = 10$ and $\Sigma_s = 2$ in the middle of the domain of the previous problem. In this case, we expect to see false diffusion where the scalar flux drops around the shadow of the absorbing material.

For each problem, the geometry is constructed manually. In general, we specify the domain of the problem as a background region to develop features on top of. For example, we include the whole rectangular domain for the isotropic source with vacuum boundary conditions, as air for the incoming beam problems, or an absorber for the small sources problem. At that point, we assign different values for the source and cross sections by determining if all nodes of a cell fall within that feature through the analytical description of the boundary. For the circular sources or absorber, this means testing whether all corners of a mesh cell falls outside a circle with the given center and radius.

2 Results

2.1 Comparison with Isotropic Source

We show the results of running our transport sweep with an isotropic source with scattering ratio 0.5 and vacuum boundary conditions in Figure 1. This solution appears spatially flat except at the edges and reaches its maximum value of 2, which agrees with our predictions and 1D testing.

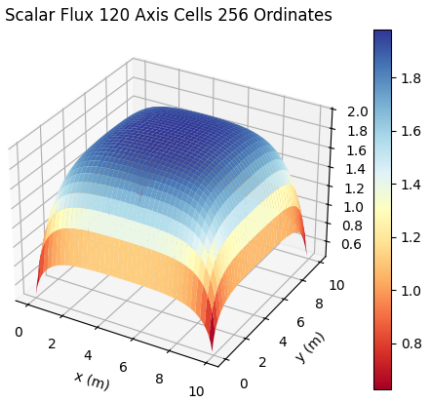

Figure 1: Simulation of a 2D isotropic source with vacuum boundary conditions. This shows qualitative and quantitative agreement with our 1D expectations.

2.2 Evidence of Ray Effects

In several cases we are able to identify ray effects. For this system, we . In Figure 2, we show the system of four isotropic sources in an absorbing domain. We can see that for a small number of angles, there are strong oscillations in the system that propagate the source far relative to its peak and even forming a peak in the center of the domain. The reason for the ray effects in this case is that many rays in this problem are unable to pass through the sources which leads to a worse average of the scalar flux. When more rays are included, the correct behavior is recovered and the four peaks are isolated. However, we observe oscillations in the background scalar flux at the same location of the earlier oscillations. This makes sense because ray effects tend to persist after increasing the angular flux.[3]

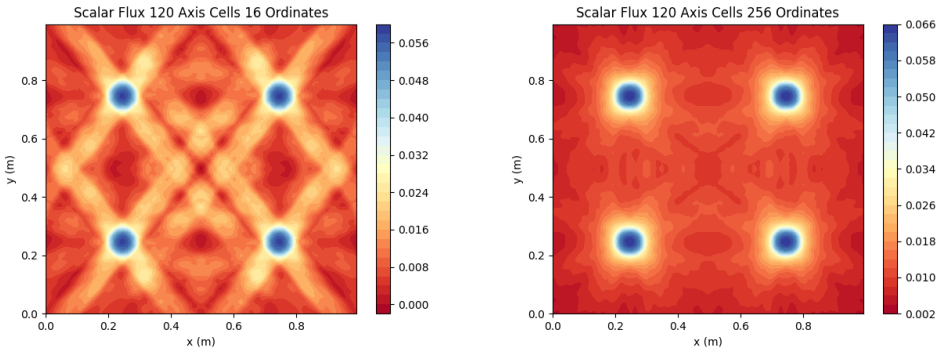

Figure 2: Scalar flux of two simulations with four 10 cm circular sources placed at (25 cm, 25 cm), (75 cm, 25 cm), (25 cm, 75 cm), and (75 cm, 75 cm). The first simulation with 16 ordinates shows strong evidence of ray effects as demonstrated by the clearly visible increases in flux for certain angles. The second with 256 ordinates shows clearly diminished oscillations, but ray effects are still visible through small patterns.

We also have a more subtle example of ray effects when considering an incident beam in 3. In a case with just four μ and ϕ values, we anticipate to see two beams instead of one because we initialize with the largest value of μ - this is a feature of our input. We even see two beams emerge at the end of the plot with 16 values each because of the constraint of our quadrature set. However, the rapid oscillations within the beam are due to the sensitive angular dependence of the angular flux.

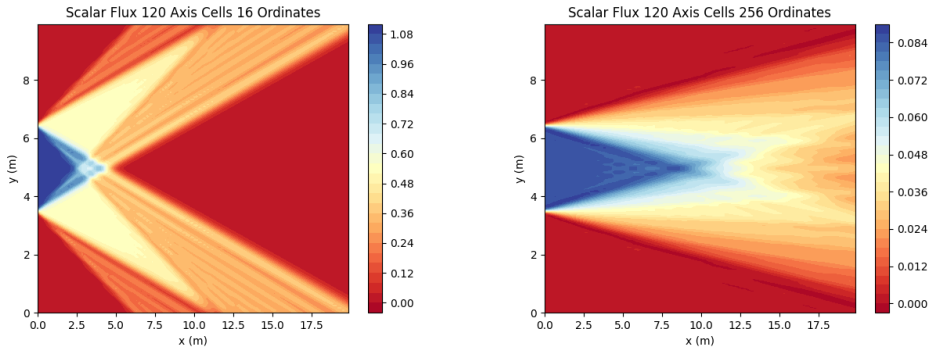

Figure 3: Scalar flux in two simulations with a beam of incident particles with largest μ. Notice the oscillations along each beam caused by ray effects.

2.3 False Diffusion

We consider an extension of our system with incident flux and add an absorber in front of the beam in Figure 4. Based on this picture, the shadow behind the absorber has a width to its edge as we see an increase and decrease in the brightness of the beam next to the shadow. This allows us to identify false diffusion.

2.4 Convergence of Solutions

We now test the convergence of our solutions for the isotropic source, four sources, incident flux, and blocked incident flux systems to the most resolved simulation of that type (120 spatial cells on each axis and 16 angular variables each). For each simulation, we adjusted the threshold of our source iteration method to be 10^{-10} to prevent that error from addressing this study.

Figure 5 shows the L^2 error in the scalar flux at shared spatial locations between solutions for each problem for varying All simulations were performed with 16 μ and ϕ variables. We see that the isotropic source error seems to decrease proportionally to the width of each cell, which we would expect from a diamond difference solution. However, each of the other problems shows that the error levels off at around 10^{-5}.

On the other hand, we investigate the convergence of a simulation in the number of ordinates in each variable for a fixed resolution of 120 cells in each direction. This leads to the results of Figure 6, where we see that in every simulation the discrepancy with the most resolved simulation

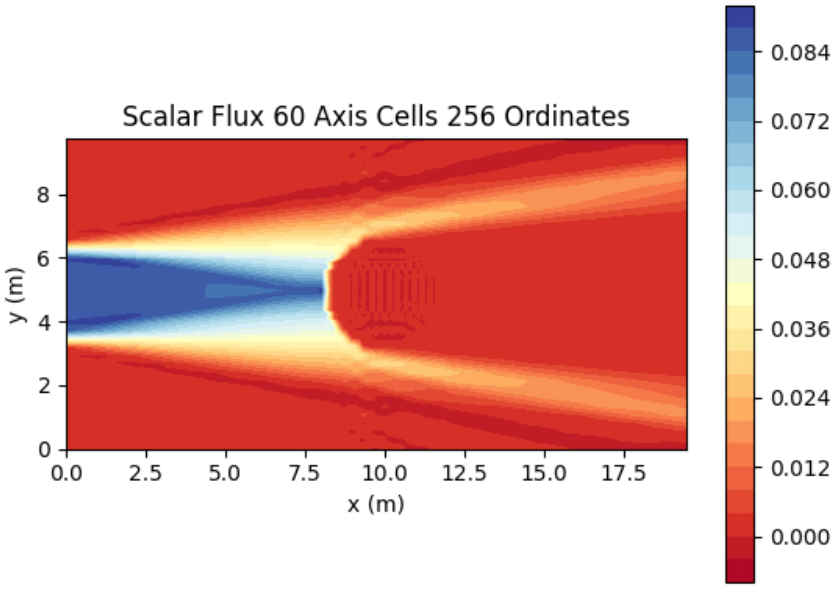

Figure 4: Scalar flux of a simulation with a beam of incident particles with large μ absorbed by an cylindrical post. We observe false diffusion based on the width where the scalar flux decreases behind the post.

appears to decrease linearly. As suggested by the previous analysis, this suggests that ray effects prevent our solutions from fully converging in the problems with localized sources.

3 Future Work

This project has illustrated some useful properties and limitations of a diamond difference approximation to the 2D transport equation. Further time and resources permitting, this work would explore how to better design a mesh using triangular cells. This would allow a sharper approximation to the circular sources and absorbing walls implemented in addition to increasing the order of convergence of this method. Based on Lewis and Miller, additional linear variation in the scalar flux throughout a cell would need to be accounted for. Use of triangular cells and a more general mesh design than the hard-coded problems studied here would allow a generalization of this code and have stronger convergence properties.

Further analysis would compare these results the problem of neutron flow past an obstruction using the method of characteristics. The method of characteristics is not limited by the need to assign values of the cross sections to a specific cell and can obtain an analytic solution. Consequently, it can achieve higher orders of convergence to a solution in a complicated geometry.

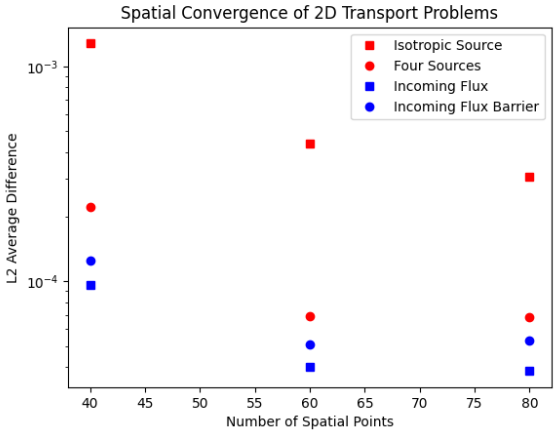

Figure 5: L^2 average discrepancy between system simulations with varying numbers of grid points on each axis and the most resolved simulation of that problem.

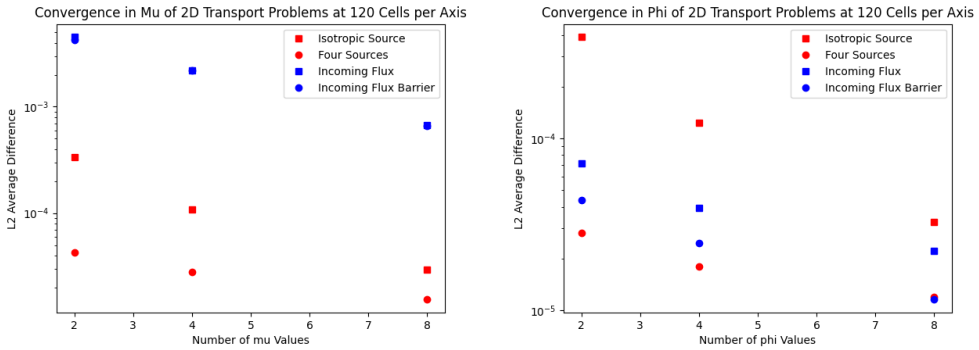

Figure 6: L^2 average discrepancy between system simulations with varying numbers of μ and ϕ ordinates and the most resolved simulation of that problem.

More broadly, this work has focused on low scattering problems to illustrate ray effects and other anomalies in discrete ordinates codes. However, further tests of the highly scattering regime in this code are unavailable due to the large numbers of iterations it would take to test a scattering regime, which is too expensive given the mesh sizes used here. This method would be feasible with a diffusion synthetic acceleration method [1]. To implement this method, we would model the difference between the actual scalar flux and the scalar flux at a given iteration as a sum of the first two spherical harmonics - which would involve solving for a correction scalar flux and currents in the x and y direction. This requires boundary conditions for these three moments and the solution of three coupled linear equations, which has not been implemented at this time.

Acknowledgements

All code used was provided in the s25me388f_hansen GitHub repository. I also appreciated the presentation by Sree Gudala on presenting the results of a 2D method of characteristics code using

3D surface plots and attempted to model the appearance of my results on his work. I believe Sree also tested his methods of characteristics code with a source at the center of the domain and a problem like the isotropic source with vacuum boundaries. I also consulted with Max Hoffing about automated ways to design a spatial mesh and some example problems to compare.

References

[1] M. L. Adams and E. W. Larsen. Fast iterative methods for discrete-ordinates particle transport calculations. *Progress in Nuclear Energy*, 2002.

[2] T. Evans, E. Biondo, G. Davidson, S. Hamilton, S. Johnson, T. Pandya, and K. Royston. Exnihilo transport methods manual. Technical report, Oak Ridge National Laboratory, 2020.

[3] E. Lewis and W. Miller. *Computational Methods of Neutron Transport*. American Nuclear Society, 1993.